Size effects and characteristic lengths in superconducting films and interfaces

Branko P. Stojković and Oriol T. Valls
Center for the Science and Application of Superconductivity, School of Physics and Astronomy, University of Minnesota, 116 Church St. S.E., Minneapolis, Minnesota 55455-0149
(Received 8 June 1993)

We examine geometric and finite-size effects in superconductors, using a purely microscopic method. The case where the coherence length ξ_0 is short and phenomenological methods cannot be used is emphasized. We focus on the single-particle density of states, the energy gap, and the order parameter, and obtain results as a function of temperature, coherence length, system size, distance to the boundary, and pair-breaking impurity mean free path. We discuss the roles of all of the relevant lengths and the experimental implications of our results, in particular, how data from surface probes can yield information on bulk properties.

I. INTRODUCTION

The study of geometric effects plays an important role in the theory of superconductivity. It is an essential bridge between the basic theoretical models, usually obtained for infinite systems with periodic boundary conditions, and experimental results obtained on finite samples, often in films, granular materials, and other confined geometries. Thus, this question has drawn a strong interest from both theorists and experimentalists for a long time.

From the development of the Bardeen-Cooper-Schrieffer[1] (BCS) theory, and extending into the late 70s, much was accomplished in the area: Several models explained quite successfully the variation of the order parameter (OP) function $\Delta(\mathbf{r})$ near superconductor-normal metal (SN) and superconductor-insulator (SI) interfaces, the properties of superconducting thin films, tunneling data, critical current measurements on small samples, etc. These results[2] relied heavily on the Ginzburg-Landau (GL) phenomenological theory, or on non-self-consistent solutions[3,4] of the microscopic Gor'kov equations[5] (GE). Such approaches were, in general, satisfactory for the case of ordinary metallic superconductors, such as aluminum or tin, due to the long superconducting coherence length ξ_0 of these materials (e.g., $\xi_0 \approx 16\,000$ Å for aluminum).[6] During that period, the fact that ξ_0 is much larger than the characteristic microscopic lengths, such as the Fermi wavelength in ordinary superconductors, was used as a given, explicitly or implicitly, in treatments of interface, boundary, and geometrical effects.

The discovery of high-temperature superconductivity[7] brought new attention to this subject. The coherence length ξ_0 of high-temperature superconductors (HTSC's) has been found to be quite short compared to that in ordinary superconductors, and the condition $k_F\xi_0 \gg 1$ does not hold. The entire area of size and interface effects was, therefore, found to be in need of reexamination: For example, as first pointed out by Deutscher and Müller,[8] the straightforward application of GL based theory to the case of short ξ_0 superconductors would entail a drastic depletion of the OP near SI interfaces over an extended temperature range. We have recently shown,[9] by using a purely microscopic and fully self-consistent theory, that the results of standard GL based methods could indeed be seriously in error. In particular, the severe depletion of the OP function near a SI interface in short ξ_0 superconductors, discussed in Ref. 8, is not found in the microscopic calculation: it is much smaller, and occurs only at temperatures extremely close to T_c. The results in Ref. 9 (in particular from Figs. 6–8 there) indicate that, although there is a length $\xi(T)$, increasing as $T \to T_c$, associated with the OP behavior, this is not the only length associated with the function $\Delta(\mathbf{r})$ near the interface. Thus, one cannot use the single GL coherence length $\xi_{\rm GL}(T)$ to phenomenologically describe interfaces.

Experimentally, this issue is important because tunneling, the usual probe of the quasiparticle spectrum, is a surface probe. For small ξ_0, high-T_c materials it gains additional importance because photoemission, also a surface probe, can be used as well. Photoemission experiments[10] indicate the existence of a considerable gap (large in comparison with k_BT_c) near the interface. There are a number of reports[11] of tunneling results in the basal plane of high-T_c materials also showing a substantial gap, in agreement with photoemission. The values found are also consistent with those obtained from a "small gap" interpretation[12] of infrared measurements, although other interpretations indicating no gap[13] or a much larger gap are also possible and make this a still controversial issue. An abrupt variation of the OP near a SN interface has also been found[14] using scanning tunneling microscopy (STM). While one can argue about the results of any single technique, in our opinion the cumulative experimental evidence against a universal and severe gap depletion at the surface is very strong.

However, many of the experimental implications of the OP behavior remain unexplored. In particular, one has to determine the relationship between the local value of the OP in a sample, and the value of the energy gap in the single-particle spectrum. Given that tunneling probes a sample only within a few coherence lengths of the surface,

how is the measured gap related to that which one would find in the bulk? For large ξ_0 superconductors, this issue was examined some time ago.[15] It was concluded that the measured gap would be the minimum value of the OP in the sample, coarse grained over a distance ξ_0. For short ξ_0 superconductors, it was tacitly assumed that normal edge states would appear in the tunneling spectrum.

In this work we attempt a careful reexamination of these questions. We focus on interface effects on the density of states (DOS). We calculate the DOS for short ξ_0 superconductors for the case of finite geometry consisting of a slab of thickness d. When d is sufficiently large, the behavior of most of the sample is in the bulk regime, while the presence of the interfaces is still felt in the region near the surface. We use the same purely microscopic methods as in Ref. 9 to calculate the OP and the DOS. We have also included the effect of pair breaking impurities, using an extension of the usual Abrikosov[16] method to our geometry. Our objective is to sort out the roles of different characteristic lengths in the problem: the coherence lengths, the mean free path l, the Fermi wavelength $\lambda_F = 2\pi/k_F$ (k_F is the Fermi wavevector), the distance z from the surface, and the thickness d. The method we use shows many important features of interface and finite-size effects and all of their complexity.

It follows from our results that the energy gap as measured in tunneling experiments should be close to the bulk value of the OP function $\Delta(z)$ even for small ξ_0. Only a very slight reduction due to surface effects should occur. The DOS for the geometry we consider represents the single-particle states of the system over a region of extended depth. We find, however, that it should be possible to extract information on finite-size effects from tunneling data on samples of finite thickness d, even though these effects are not large. We discuss the interplay between the length scale for OP variations and sample thickness, in both the clean and dirty cases. We also find that the transition temperature of finite-size short ξ_0 superconductors depends on l in the same way as the bulk T_c, and is monotonic in d, while on the other hand, T_c for finite l and long ξ_0 superconductors exhibits quantum oscillations, as in the clean case.[9,17]

This paper is organized as follows: in Sec. II we review our formulation of the Gor'kov equations, which we use to obtain self-consistent results. We introduce our method of solution, and of extracting the DOS. We explain the modifications to the self-energies in finite geometries, and the inclusion of a finite mean free path. In Sec. III we present and analyze our results. Finally a summary discussion of the results is in Sec. IV.

II. MODEL

In this section we review the methods we use.[9] We consider a system confined to the region $0 < z < d$, and infinite in the x, y directions (slab geometry). We emphasize the details of the calculation of the DOS, and also show how to include impurities self-consistently in finite geometry.

Our starting point is the standard Gor'kov equations,[18] with a contact pairing interaction acting between electrons within energy range ω_0 from the Fermi surface. The nature of the interaction is unspecified. In the slab geometry one finds it convenient[9] to perform a spatial Fourier transform in the x, y plane, and to expand the normal and anomalous Green's functions G and F, in terms of the complete set of eigenfunctions $u_\nu(z)$ of a one-dimensional box. Thus,

$$G(z,z',k_\perp,\omega_n) = \sum_{\nu\nu'} u_\nu(z)\, u_{\nu'}(z')\, g_{\nu\nu'}(k_\perp,\omega_n), \quad (2.1a)$$

$$F^\dagger(z,z',k_\perp,\omega_n) = \sum_{\nu\nu'} u_\nu(z)\, u_{\nu'}(z')\, f^*_{\nu\nu'}(k_\perp,\omega_n), \quad (2.1b)$$

where

$$u_\nu(z) = \langle z|\nu\rangle = \sqrt{\frac{2}{d}}\,\sin(k_\nu z), \qquad k_\nu \equiv k_z = \frac{\nu\pi}{d}, \quad (2.2)$$

$\mathbf{k}_\perp$ is the wave vector in the transverse direction (x, y plane), and ω_n are the Matsubara frequencies. As discussed in Ref. 9, this expansion is appropriate provided $k_F d$ is not too small, so that electronic wave function "leak" outside the sample[19] can be neglected. For thin films there may be other problems related to modifications of the electron pairing interaction.[20] At zero magnetic field $\Delta(\mathbf{r})$ is effectively only a function of z, the distance from the interfaces, and one can expand:

$$\Delta(z) = \sum_{\nu}^{N} u_\nu(z)\,\Delta_\nu. \quad (2.3)$$

The upper limit N of the sum in Eq. (2.3) is determined by the range of the pairing interaction ω_0: the energy of a particle with a wave vector $\mathbf{k} \equiv (k_\nu, \mathbf{k}_\perp)$ must lie in the region $(E_F - \omega_0,\, E_F + \omega_0)$ about the Fermi surface. We consider a system with constant carrier density, therefore the chemical potential μ is a function of thickness d.[17,21] We also assume that the Fermi energy E_F is approximately equal to the chemical potential μ. Thus,

$$N = \left[\frac{k_F d}{\pi}\sqrt{1+\frac{\omega_0}{E_F}}\,\right], \quad (2.4)$$

where square brackets denote the integer part. The sums in Eqs. (2.1) extend formally to infinity. However, since both Δ and $F^\dagger$ are non-zero only in the mentioned region near the Fermi surface, outside this region $g_{\nu\nu'}$ reduces to its normal metal limit:[16,22]

$$g_{\nu\nu'}(k_\perp,\omega_n) = \delta_{\nu\nu'}\,\frac{1}{i\omega_n - \xi_\nu}, \quad (2.5)$$

where $\xi_\nu = k_\perp^2/2m + k_\nu^2/2m - \mu$. In practice, values of ν and ν' much larger than N are not needed for convergence in the energy scales we study.

If we define appropriate matrices $\underline{G}$, $\underline{F}$, $\underline{C}$, and $\underline{X}$, with matrix elements:

$$\begin{aligned} G_{\beta\rho} &\equiv g_{\beta\rho}(k_\perp,\omega_n), & F_{\beta\rho} &\equiv f^*_{\beta\rho}(k_\perp,\omega_n), \\ C_{\beta\rho} &\equiv \sum_\nu \Delta_\nu\, J_{\nu\beta\rho}, & X_{\beta\rho} &\equiv \xi_\beta\,\delta_{\beta\rho}, \end{aligned} \quad (2.6)$$

where

$$J_{\nu\nu'\beta} = \int_0^d dz\, u_\nu(z)\, u_{\nu'}(z)\, u_\beta(z), \tag{2.7}$$

then it is easy to see that the Gor'kov equations become matrix equations, completely analogous to their bulk Fourier transforms. One easily finds their formal solution:

$$\underline{F} = \left[\underline{C} - (i\omega_n - \underline{X})\,\frac{1}{\underline{C}^*}\,(i\omega_n + \underline{X})\right]^{-1} \tag{2.8}$$

and

$$\underline{G} = -\frac{1}{\underline{C}^*}\,(i\omega_n + \underline{X})\,\underline{F} \tag{2.9a}$$

$$= \left[i\omega_n - \underline{X} - \underline{C}\,\frac{1}{i\omega_n + \underline{X}}\,\underline{C}^*\right]^{-1}, \tag{2.9b}$$

with the self-consistency (gap) equation:

$$\Delta_\beta^* = gT \sum_{\nu\nu'} J_{\nu\nu'\beta} \int \frac{d^2k_\perp}{(2\pi)^2} \sum_n F_{\nu\nu'}. \tag{2.10}$$

Here g is the bulk coupling constant, T is the temperature. We have taken $k_B = \hbar = 1$. The matrix $\underline{C}$, and therefore the matrices $\underline{F}$ and $\underline{G}$ as well, are symmetric.

Our method consists of solving Eqs. (2.8) and (2.9) numerically. The computations are simplified if one recalls that, as discussed in Ref. 9, the matrix $\underline{C}$, and therefore the matrices $\underline{F}$ and $\underline{G}$, are approximately diagonal both at large and small $k_F d$, which makes the matrix inversions in Eqs. (2.8) and (2.9) somewhat easier. Writing then

$$\underline{C} = \underline{D} + \underline{O}, \tag{2.11}$$

where $\underline{D}$ is the large, diagonal part, and $\underline{O}$ is the small, off-diagonal part of $\underline{C}$, and expanding Eqs. (2.8) and (2.9) in terms of $\underline{O}$, one obtains the formal expansion for $\underline{F}$:

$$\begin{aligned}\underline{F} = {} & \frac{\underline{D}}{{\omega_n}^2 + \underline{X}^2 + \underline{D}^2} - \frac{\underline{D}}{{\omega_n}^2 + \underline{X}^2 + \underline{D}^2}\,\underline{\Theta}\,\frac{\underline{D}}{{\omega_n}^2 + \underline{X}^2 + \underline{D}^2} \\ & + \frac{\underline{D}}{{\omega_n}^2 + \underline{X}^2 + \underline{D}^2}\,\underline{\Theta}\,\frac{\underline{D}}{{\omega_n}^2 + \underline{X}^2 + \underline{D}^2}\,\underline{\Theta}\,\frac{\underline{D}}{{\omega_n}^2 + \underline{X}^2 + \underline{D}^2} - \cdots,\end{aligned} \tag{2.12}$$

where

$$\underline{\Theta} = \underline{O} + (i\omega_n - \underline{X})\left(\underline{D}^{-1}\underline{O}\,\underline{D}^{-1}\right)\frac{1}{1 + \underline{O}\,\underline{D}^{-1}}\,(i\omega_n + \underline{X}). \tag{2.13}$$

There is also an equivalent expansion for the normal Green's function G.

It is important to realize that the solution (2.12) contains only superconducting excitations of the system: by analytically continuing G and F onto the real frequencies ($i\omega_n \to E$), and recalling Eqs. (2.9a) and (2.12), one sees that there are no normal metal low-energy poles where Δ is nonzero. Then to first order in $\underline{O}$ we have:

$$\Delta_\beta = gT \sum_{\nu\nu'} J_{\nu\nu'\beta} \int \frac{d^2k_\perp}{(2\pi)^2} \sum_n \left[\frac{C_{\nu\nu}}{{\omega_n}^2 + {\xi_\nu}^2 + C_{\nu\nu}^2}\,\delta_{\nu\nu'} + (1 - \delta_{\nu\nu'})\,\frac{{\omega_n}^2 + \xi_\nu\xi_{\nu'} - C_{\nu\nu}C_{\nu'\nu'}}{({\omega_n}^2 + {\xi_\nu}^2 + C_{\nu\nu}^2)({\omega_n}^2 + {\xi_{\nu'}}^2 + C_{\nu'\nu'}^2)}\,C_{\nu\nu'}\right]. \tag{2.14}$$

Here we have omitted terms which vanish by symmetry when performing sums over Matsubara frequencies. Equation (2.14) is the self-consistency equation, the analog of the gap equation in the bulk case. It is easily confirmed that as expected from the Gor'kov equations, the order parameter $\Delta(z)$ and its components Δ_β from Eq. (2.14) can be assumed to be real without loss of generality. Therefore we have written $\underline{C} = \underline{C}^*$.

Performing the analytic continuation for G, i.e., $G(z, z', k_\perp, i\omega_n) \to G(z, z', k_\perp, E)$, one finds, to first order in $\underline{O}$,

$$\underline{G} \approx \frac{E + \underline{X}}{E^2 - (\underline{X}^2 + \underline{D}^2)} + \frac{1}{E^2 - (\underline{X}^2 + \underline{D}^2)}\,[\underline{D}\,\underline{O}\,(E + \underline{X}) + (E + \underline{X})\,\underline{O}\,\underline{D})]\,\frac{1}{E^2 - (\underline{X}^2 + \underline{D}^2)}, \tag{2.15}$$

and finally

$$G(z, z', k_\perp, E) = \sum_{\nu\nu'} u_\nu(z) u_{\nu'}(z') \left[\frac{E + \xi_\nu}{E^2 - (\xi_\nu^2 + C_{\nu\nu}^2)}\,\delta_{\nu\nu'} + (1 - \delta_{\nu\nu'})\,\frac{C_{\nu\nu}(E + \xi_{\nu'}) + (E + \xi_\nu)C_{\nu'\nu'}}{(E^2 - \xi_\nu^2 - C_{\nu\nu}^2)\,(E^2 - \xi_{\nu'}^2 - C_{\nu'\nu'}^2)}\,C_{\nu\nu'}\right]. \tag{2.16}$$

Equation (2.14) must be solved numerically, using an iteration procedure. We start with an appropriate choice for Δ_β's, calculate the matrix $\underline{C}$ from the definition (2.6), and obtain new Δ_β's. We stop the procedure when the relative change in $\Delta(z)$ $(0 < z < d)$, between two successive iterations, is less than 1×10^{-4}.

We can now use Eq. (2.16) to obtain the DOS. We define the quantity[23]

$$N(z, k_\perp, E) = -\frac{1}{\pi} \operatorname{Im} G(z, z, k_\perp, E + i\varepsilon), \tag{2.17}$$

where ε is a positive infinitesimal. The DOS can then be found by integrating $N(z, k_\perp, E)$ over the appropriate range of $\mathbf{k}_\perp$ and z.

The above calculation applies only to pure samples, and we now introduce random impurity scattering in the calculation. We assume that the impurity potentials $W(\mathbf{r})$ are weak, which allows us to use a perturbation expansion, quite analogous to the well-known methods of Abrikosov *et al.*,[16] for the treatment of impurity scattering in bulk superconducting alloys. We are also interested only in the Green's functions averaged over impurity positions. In this case the matrix Gor'kov equations become

$$[i\omega_n - \underline{X} - \underline{\Sigma}^G(i\omega_n)]\,\underline{G} + (\underline{C} - \underline{\Sigma}^F)\,\underline{F} = 1, \tag{2.18a}$$

$$[i\omega_n + \underline{X} + \underline{\Sigma}^G(-i\omega_n)]\,\underline{G} + (\underline{C} - \underline{\Sigma}^F)\,\underline{F} = 1, \tag{2.18b}$$

where $\underline{\Sigma}^G$ and $\underline{\Sigma}^F$ are the impurity self-energies involved. We have assumed here that the impurities are pair breaking. If they are not, $\underline{\Sigma}^F$ takes a plus sign in Eq. (2.18).

In the slab geometry, the self-energies are also matrices. We make the following assumptions: we need $\underline{\Sigma}^F$ and $\underline{\Sigma}^G$ only to first order in $(1/k_F d)^2$, since we are not considering thin films where $k_F d \sim 1$. We then make the usual assumption that the impurities are dilute ($k_F l \gg 1$, where l is the mean free path) and that the impurity potential is completely screened at distances of order of several k_F^{-1}, resulting in

$$W(\mathbf{r}) = W(r) \to 0, \quad |\mathbf{r}| \lesssim \frac{\pi}{k_F}. \tag{2.19}$$

Here we have also assumed that the impurity potential is spherically symmetric. Our final assumption is that there is no correlation between the impurity positions and the location of the boundaries.

From these considerations, it follows that it is sufficient to calculate the matrices $\underline{\Sigma}^F$ and $\underline{\Sigma}^G$ within the diagonal approximation. Off-diagonal terms would introduce corrections of higher order in $(1/k_F d)^2\,(1/k_F l)$. This quantity is not necessarily negligible in the calculations of the OP in HTSC's. However, since impurity potentials are weak, and their self-energies are effectively only corrections to the Green's functions (calculated to second order in the Born approximation), the error associated with the exclusion of these terms will be much smaller than the self-energies, and can therefore be neglected.

Thus, one finds

$$\Sigma^G_{\beta\rho}(\mathbf{k}_\perp, i\omega_n) = \delta_{\beta\rho} \int d\xi'_\beta\, \tilde{W}(z, \mathbf{k}_\perp, \mathbf{k}_\perp{}')\, g_{\beta\beta}(k_\perp{}', \tilde{\omega}_n), \tag{2.20a}$$

$$\Sigma^F_{\beta\rho}(\mathbf{k}_\perp, i\omega_n) = \delta_{\beta\rho} \int d\xi'_\beta\, \tilde{W}(z, \mathbf{k}_\perp, \mathbf{k}_\perp{}')\, f^*_{\beta\beta}(k_\perp{}', \tilde{\omega}_n), \tag{2.20b}$$

where $i\tilde{\omega}_n$ is defined below and

$$\tilde{W}(z, \mathbf{k}_\perp, \mathbf{k}_\perp{}') = N_i \frac{m k_F}{2\pi^2 d} \int dz_i\, d\varphi\, [W(z - z_i, \varphi)]^2\,. \tag{2.21}$$

Here N_i is the number of impurities, and φ is the angle between $\mathbf{k}_\perp$ and $\mathbf{k}_\perp{}'$. In Eqs. (2.20) the same restrictions apply as in Abrikosov theory, i.e., all vectors must be near the Fermi surface. With this and the other conditions discussed above, $\tilde{W}$ from Eq. (2.21) obviously does not depend either on $\mathbf{k}_\perp$, nor on z and in the limit $d \to \infty$ it becomes identical to the bulk impurity scattering rate $1/2\tau$. As discussed above, we can neglect corrections of order $(1/k_F d)^2$, and simply conclude $\tilde{W} \approx 1/2\tau = v_F/2l$, where v_F is the Fermi velocity.

We then write

$$i\underline{\tilde{\omega}} = i\omega_n - \underline{\Sigma}^G, \qquad \underline{\tilde{C}} = \underline{C} - \underline{\Sigma}^F \tag{2.22}$$

(where a Matsubara index in $i\underline{\tilde{\omega}}$ is suppressed for clarity) and obtain a solution for the Green's functions formally identical to (2.8) and (2.9), except that $i\underline{\tilde{\omega}}$ replaces $i\omega_n$, and $\underline{\tilde{C}}$ replaces $\underline{C}$. After performing the necessary integrations we find for the diagonal elements of $\underline{\tilde{\omega}}$ and $\underline{\tilde{C}}$ explicitly:

$$\tilde{\omega}_{\nu\nu} = \omega_n + \frac{1}{2\tau} \frac{\tilde{\omega}_{\nu\nu}}{\sqrt{\tilde{\omega}^2_{\nu\nu} + \tilde{C}^2_{\nu\nu}}}, \tag{2.23a}$$

$$\tilde{C}_{\nu\nu} = C_{\nu\nu} - \frac{1}{2\tau} \frac{\tilde{C}_{\nu\nu}}{\sqrt{\tilde{\omega}^2_{\nu\nu} + \tilde{C}^2_{\nu\nu}}}. \tag{2.23b}$$

If nonpair breaking impurities are also present, with a scattering time τ_N, then $1/\tau$ must be replaced by $(1/\tau + 1/\tau_N)$ in Eq. (2.23a), and by $(1/\tau - 1/\tau_N)$ in Eq. (2.23b).

The self-consistency equation (2.14) finally becomes

$$\Delta_\beta = gT \sum_{\nu\nu'} J_{\nu\nu'\beta} \int \frac{d^2 k_\perp}{(2\pi)^2} \sum_n \left[\frac{\tilde{C}_{\nu\nu}}{\tilde{\omega}^2_{\nu\nu} + \xi^2_\nu + \tilde{C}^2_{\nu\nu}} \delta_{\nu\nu'} + (1 - \delta_{\nu\nu'}) \frac{\tilde{\omega}_{\nu\nu}\tilde{\omega}_{\nu'\nu'} + \xi_\nu \xi_{\nu'} - \tilde{C}_{\nu\nu}\tilde{C}_{\nu'\nu'}}{(\tilde{\omega}^2_{\nu\nu} + \xi^2_\nu + \tilde{C}^2_{\nu\nu})(\tilde{\omega}^2_{\nu'\nu'} + \xi^2_{\nu'} + \tilde{C}^2_{\nu'\nu'})} C_{\nu\nu'} \right]. \tag{2.24}$$

In order to obtain the DOS we now perform the analytic continuation from Matsubara frequencies to the real energies. This is not as straightforward as in the clean case, and requires the definition of a real energy array $\underline{\tilde{E}}$:

$$\tilde{E}_\nu = E + \frac{1}{2\tau}\frac{i\tilde{E}_\nu}{\sqrt{\tilde{E}_\nu^2 - \tilde{C}_{\nu\nu}^2}}. \tag{2.25}$$

One then obtains the expression for the DOS in the dirty case:

$$N(z,k_\perp,E) = -\frac{1}{\pi}\,\mathrm{Im}\sum_{\nu\nu'} u_\nu(z)u_{\nu'}(z)\left[\frac{\tilde{E}_\nu+\xi_\nu}{\tilde{E}_\nu^2-(\xi_\nu^2+\tilde{C}_{\nu\nu}^2)}\delta_{\nu\nu'} + (1-\delta_{\nu\nu'})\frac{\tilde{C}_{\nu\nu}(\tilde{E}_{\nu'}+\xi_{\nu'}) + (\tilde{E}_\nu+\xi_\nu)\tilde{C}_{\nu'\nu'}}{(\tilde{E}_\nu^2-\xi_\nu^2-\tilde{C}_{\nu\nu}^2)(\tilde{E}_{\nu'}^2-\xi_{\nu'}^2-\tilde{C}_{\nu'\nu'}^2)}C_{\nu\nu'}\right], \tag{2.26}$$

which is the equivalent of Eqs. (2.16) and (2.17) in the presence of impurities.

Prior to the solution of Eqs. (2.24) and (2.26) one must solve Eqs. (2.23) for each value of ν, which we did numerically. We performed the integration in Eq. (2.24) analytically, and the sum over Matsubara frequencies numerically. The integrals over $\mathbf{k}_\perp$ required to obtain DOS were also obtained analytically.

III. RESULTS

In this section we present the results of our model. First we emphasize geometric effects in clean systems, i.e., the interplay of thickness and coherence length. We then introduce pair breaking disorder. We present results for the DOS [including the energy gap and its relation to $\Delta(z)$], and the OP as a function of temperature, thickness, and geometry. We also discuss the shape of the OP near a surface in dirty systems, and the transition temperature.

The physical parameters of our model are the characteristic cutoff frequency ω_0, the zero-temperature bulk OP in a pure superconductor Δ_0, the Fermi energy E_F, the thickness of the slab d, the mean free path for pair breaking impurities l, and the temperature T. However, since several of the physical parameters are not independent of each other, one only needs to consider some dimensionless ratios. We choose the same dimensionless parameters as in Ref. 9: $k_F\xi_0$, k_Fd, Δ_0/ω_0, and $t \equiv T/T_c$, with the addition of k_Fl. The chemical potential μ is calculated as a function of d. The value of $k_F\xi_0$ is related to that of T_F/T_c by $k_F\xi_0 \approx 0.36\,(T_F/T_c)$.

We have used for these dimensionless parameters values relevant to several experimental situations. Thus, we have chosen $\pi k_F\xi_0 = 20\,000$ and $\pi k_F\xi_0 = 20$ as being representative, respectively, of typical metallic superconductors such as Sn, and of short coherence length materials such as the cuprates. In the latter case, the chosen value of ξ_0 is closer to that in the basal plane. For short ξ_0 materials one must take much larger values of Δ_0/ω_0 than when ξ_0 is long.[24] Thus, we take values of Δ_0/ω_0 as high as 0.5 in the short ξ_0 case, and as low as 0.01 for long ξ_0. This is appropriate since the order of magnitude of the zero-temperature OP in HTSC's is $\sim$ 100 K, while the cutoff frequency is presumably still of the same order as in long ξ_0 materials.

Figure 1 shows the DOS calculated for a clean system of fairly large thickness $k_Fd = 750$ and long coherence length $\pi k_F\xi_0 = 20\,000$ at $T = 0$, while Fig. 2 shows the same quantity for a short ξ_0 superconductor, $\pi k_F\xi_0 = 20$, at $t = 0.45$ and for $k_Fd = 2000$. The quantity plotted is obtained from $N(z,k_\perp,E)$ as given by Eq. (2.17), summed over a small range of $\mathbf{k}_\perp$, $|\mathbf{k}_\perp| < 0.01\,k_F$, chosen from an estimated angular resolution of tunneling experiments. This would correspond to a high resolution ideal STM-type measurement[25] in the sense that we assume a very small transverse momentum distribution for the electrons. In a real STM measurement, however, one has appreciable energy resolution, and the theoretical results for $N(z,k_\perp,E)$ should be convolved with this resolution. This effect, which would lead to the smoothing out of the small wiggles in Fig. 2, is not included in our plot. The results given are normalized to the normal metal limit at high energies. The dashed line represents an integration over all values of z from 0 to d, that is, the density of states approximately equal to that in the bulk. The solid line is obtained by integrating over a region of z near the interface ($Z \equiv k_Fz < 10$), representing a typical surface measurement. The results shown indicate a gap near the surface not even marginally smaller than the bulk gap. There is no sign of any states in the gap. Indeed, one can conclude from Eqs. (2.16) and (2.17) that, in a slab geometry, this should be the case. Thus,

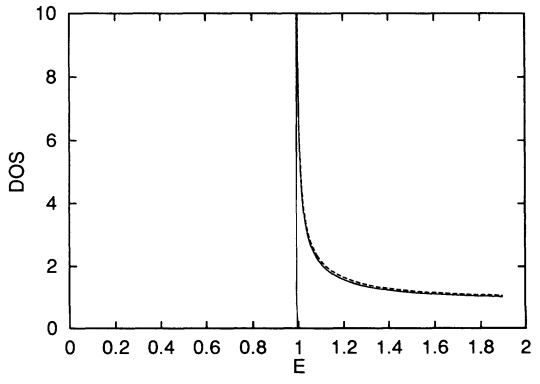

FIG. 1. The DOS for small $k_\perp$, as explained in the text, normalized to its normal bulk value, as a function of energy, measured in units of Δ_0. Here $\pi k_F\xi_0 = 20\,000$, $T = 0$, and $k_Fd = 750$. The solid line is averaged over $k_Fz < 10$, and the dashed line over all z.

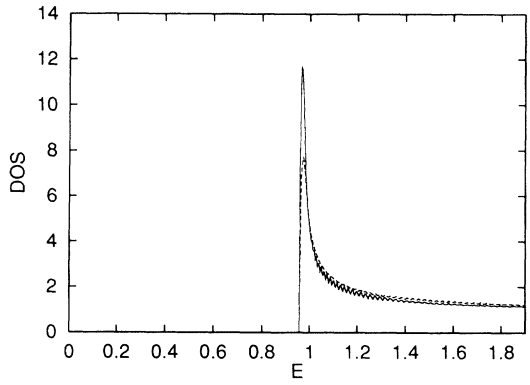

FIG. 2. As in Fig. 1, but with $\pi k_F \xi_0 = 20$, $k_F d = 2000$, and $t \equiv T/T_c = 0.45$.

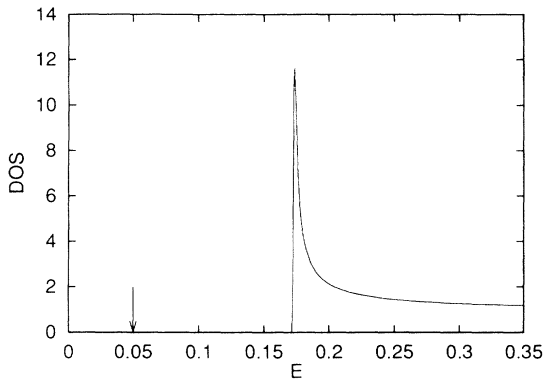

FIG. 3. Results for the DOS, for the same parameters as in Fig. 2, but a higher temperature ($t = 0.99$). Results averaged over $k_F z < 10$ are shown. The arrow indicates the gap value that one would get from phenomenological considerations (see text).

these results imply that surface probes measure the bulk density of states to a very good approximation even in short ξ_0 materials. We can say that in a superconductor without pair breaking impurities and for the geometry considered here, a probe of the density of states scans a wave function extended in the z direction,[26] therefore measuring the overall energy gap, rather than the local value of the pair potential $\Delta(z)$. The excitations are essentially similar across the system. A surface probe may well run into experimental difficulties due to the smallness of the region probed. This is definitely the case with photoemission, for example, but the measured spectrum will accurately reflect the bulk properties.

For the thicknesses considered in Figs. 1 and 2, we have that $\xi_0 \gg d$ in Fig. 1 and $\xi_0 \ll d$ in Fig. 2. Therefore, short coherence length superconductors show a more complicated finite-size structure, at higher energies, than the long coherence length ones. This is due to multiple reflections of electrons at the interfaces, which produce resonances that disappear when $d \ll \xi_0$.[4] This effect is difficult to observe experimentally at the thickness in Fig. 2, due to the above-mentioned energy resolution problems. However, as $k_F d$ decreases, one may begin to observe finite-size effects in the DOS, since when ξ_0 is small, one is never in the regime $d \ll \xi_0$. Instead of a single singularity, several can be observed, as shown below.

In Fig. 3 we use again the parameters of Fig. 2 except for a higher temperature ($t = 0.99$). We show results integrated over a region $k_F z < 10$ only. The energy gap obtained is approximately the same as the bulk order parameter at the given temperature. In contrast, if the gap is assumed to be the minimum of $\Delta(z)$ over the region considered,[15] and $\Delta(z)$ is evaluated using the phenomenological theory,[15,27] the resulting gap in the DOS is found to be much smaller, as indicated by the arrow in the figure, equal to approximately 30% of the microscopically calculated value.

In Fig. 4 we show results similar to those in Figs. 1–3, with several important differences. First, we now integrate $N(z, k_\perp, E)$ over all values of $\mathbf{k}_\perp$ (solid line). Second, we have taken here a small value of D ($D \equiv k_F d = 75$), and a temperature $t = 0.45$ so as to emphasize the finite-size effects that occur. For reference, the dashed line shows the corresponding "sharp STM" result, with $\mathbf{k}_\perp$ integrated over the range $|\mathbf{k}_\perp| < 0.01\, k_F$ (normalized in the same way), and the dotted line shows the bulk result. The range of integration for z turns out to be unimportant, the results shown are integrated over all z. Notice the energy scale shown. The DOS, integrated over all $\mathbf{k}_\perp$, in a finite-size system contains many excitation peaks. The scale of the structure shown is such that it might be experimentally resolvable in carefully performed, low field tunneling experiments. The peaks represent a "splitting" of the bulk square root singularity due to discreteness of k_z, and should not be mistaken for the higher-energy resonances (Fig. 2), which here completely disappear. This effect is also present to some extent when $|\mathbf{k}_\perp|$ is small. There, however, probes "see" only the few excitations with the minimum gap value.

The overall width of the energy region where this structure is seen, depends on ξ_0 and, through the size of the OP, on the temperature. The structure is a consequence of the dependence of $\Delta(z)$ on the discrete k_z. From Eq. (2.4) it follows that this dependence decreases as

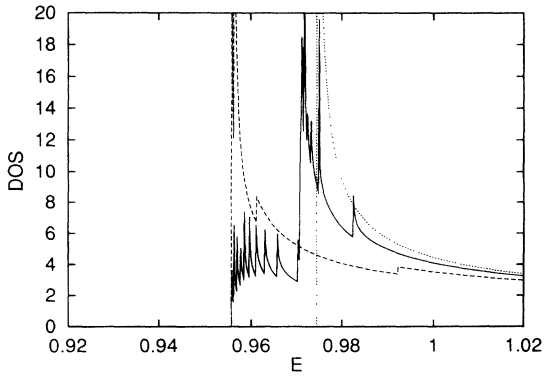

FIG. 4. The normalized DOS, integrated over all $k_\perp$ and z, for $k_F d = 75$ and $t = 0.45$ (solid line). The dashed line is integrated over small $k_\perp$, normalized in the same way. The dotted line is the bulk DOS.

$(k_F d)^{-1}$. For short ξ_0 superconductors the value of $k_F d$ used in Fig. 4, while still relatively small, is large enough so that over most of the temperature range $\xi(T) \lesssim d$, and finite-size effects occur in the wave functions corresponding to larger k_z values. The main peak in the solid line is very close to the bulk gap, and it is due to small k_z electrons. The bulk gap, obtained using standard methods[16] and indicated by the dotted line, is larger than the gap calculated here, due to the small thickness. The electrons with larger k_z produce the peaks corresponding to smaller energy values.

On the other hand, quantum finite-size effects on the *average value* of the OP and the energy gap are present in long ξ_0 superconductors, as shown by many authors both theoretically and experimentally.[17,21,28–30] However, in short ξ_0 superconductors, at any physically significant thickness, this effect is smeared out.[9] The OP in these systems should reach its bulk value from below, and that is why we see the gap slightly below its bulk value in Fig. 4. The gap there is simply the OP value averaged over the slab thickness.

It is interesting to discuss the local order parameter $\Delta(z)$ in relation to the energy gap in the spectrum, for a finite system. We begin with Fig 5. The solid line there shows $\Delta(z)$ for the same thickness as in Fig. 4, while the dashed line shows the OP in a thicker sample ($k_F d = 750$). Again, the difference between the phenomenological result, shown by the dotted line, and the microscopic solution for the OP is clearly evident. The Friedel-like oscillations should be ignored here. The flat horizontal lines correspond to the energy gap, as obtained from our calculation of the DOS for these systems. The gap is somewhat smaller for the thinner slab, but it is still considerable. In both cases it is very close to the average of $\Delta(z)$. This indicates that the results of Ref. 27 hold only if it is understood that the variations of the OP on a scale of λ_F must be averaged out. It can be seen in Fig. 5 that, as in Ref. 9, in addition to the sharp rise in $\Delta(z)$ over a short scale within $\sim k_F^{-1}$ from the interface, a smaller increase occurs within a longer, temperature dependent range $\xi(T)$. This is shown more clearly in Fig. 6 where the results for several additional temperatures are shown for the thicker of the two systems in Fig. 5. Note that the OP shown is normalized with respect to the bulk OP $\Delta(T)$ at each given temperature. The results obtained at different temperatures are shifted by a multiple of $0.2 \times \Delta(T)$ for clarity. One can see that, as the temperature approaches T_c, the depletion of the OP at the interface becomes gradually more prominent. We have found that the larger length associated with this variation of the OP is $\xi(T) \sim (1-t)^{-\alpha}$, with $\alpha \simeq 1/2$ as expected, provided that $k_F d > \xi(T)$.

Figures 5 and 6 show that, although the OP in short ξ_0 materials exhibits a small variation over long length scales at temperatures close to T_c, near a SI interface, most of the change takes place over a short distance. One cannot describe the overall behavior by a *single* coherence length $\xi_{GL}(T)$.[31] The reason for this discrepancy between microscopic and phenomenological results is quite obvious: the basic assumption of all GL based theories is that the variation of the OP is very small over a range much larger than the interatomic distance. In other words, the OP near a SI interface, in the absence of a magnetic field, should satisfy the boundary condition

$$\frac{d}{dz}\Delta(z) = 0 \tag{3.1}$$

to a good approximation. The boundary condition (3.1) assumes implicitly that terms involving, e.g., the first derivative of the OP, do not contribute to the free energy functional even near the interface. This was found to be approximately correct microscopically[2] for the case of long ξ_0 superconductors, but, as discussed above, the OP should exhibit, according to GL theories, a significant variation near the interface in the case of short ξ_0 superconductors. In that case Eq. (3.1) is no longer satisfied, and therefore the original GL free energy functional is not applicable near the interface. This is why a purely microscopic approach must be used.

The value of T_c as a function of d is given in Fig. 7.

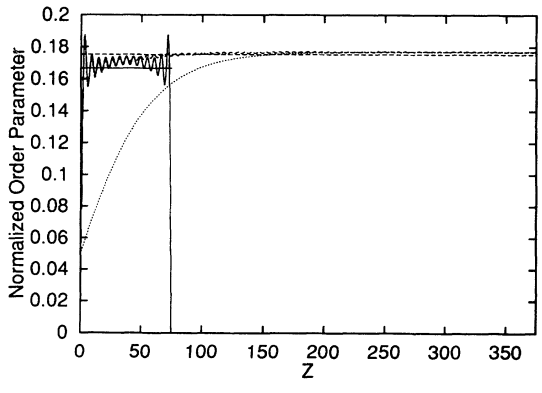

FIG. 5. The normalized OP $\Delta(z)/\Delta_0$ vs $Z \equiv k_F z$ for a clean system, at $t = 0.99$, $\pi k_F \xi_0 = 20$. The solid curve is for $k_F d = 75$ and the dashed curve is for $k_F d = 750$. The horizontal flat lines represent the corresponding energy gaps obtained from the DOS calculations. The dotted line is the GL based result for the larger thickness.

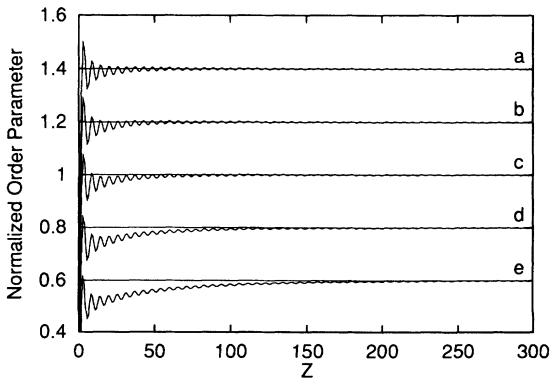

FIG. 6. Temperature dependence of $\Delta(z)$: The curves show the OP normalized to $\Delta_{\rm bulk}(T)$ at temperatures (from top to bottom) $t = 0.8, 0.9, 0.95, 0.99, 0.999$. The curves have been shifted by a multiple of 0.2. The horizontal lines are guides to the eye.

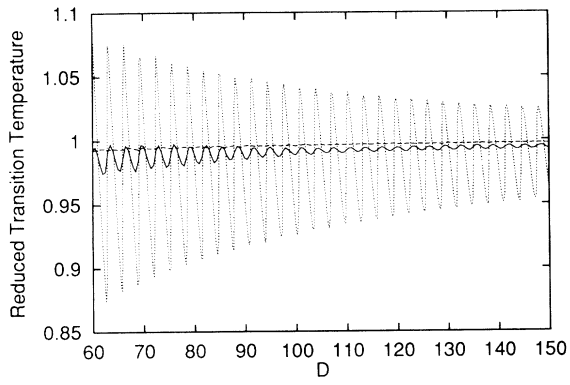

FIG. 7. $T_c(d)/T_c(\infty)$ vs $D \equiv k_F d$, for a clean system. Results are shown for $\pi k_F \xi_0 = 20$ (dashed line), $\pi k_F \xi_0 = 20\,000$ (dotted line), and $\pi k_F \xi_0 = 200$ (solid line).

We plot there T_c versus d for three values of the coherence length. One can see that for small ξ_0, T_c is indeed only very weakly dependent on the thickness, while at large values of ξ_0 we recover the well-known[17] oscillatory behavior.

We now consider the effect of adding pair breaking impurities to our system. The first question is to investigate the validity of the $d \to \infty$ formula at finite d for T_c as a function of mean free path l.[32] We write

$$-\ln\frac{T_c(d)}{T_c^0(d)} = \Psi\left(\frac{1}{2} + \frac{v_F}{2\pi l T_c(d)}\right) - \Psi\left(\frac{1}{2}\right), \qquad (3.2)$$

where $T_c^0(d)$ is the transition temperature for the clean system and Ψ is the digamma function.

We obtain T_c in the same way as in Refs. 9 and 33, by solving for the lowest eigenvalue of a system of equations [see Ref. 9, Eq. (3.4)]. The results for T_c as a function of l are given in Fig. 8 for several values of d, and $\pi k_F \xi_0 = 20$. T_c obviously obeys Eq. (3.2) to a good approximation. This equation can then be understood as a "scaling relation" between $T_c(d)$ and $T_c^0(d)$. One does find, however, deviations from this scaling law. We calculated T_c as a function of d and l. At small ξ_0 we conclude that, although T_c depends only weakly on d, thinner samples are slightly more sensitive to pair breaking scattering. This can be seen in the inset of Fig. 8 and it can be understood as arising from the destruction of superconductivity when $\xi(T) \gtrsim d$, as discussed above. This is also related to the decrease of the energy gap as d decreases (Fig. 5) and the behavior of $T_c(d)$ in pure films (Fig. 7).

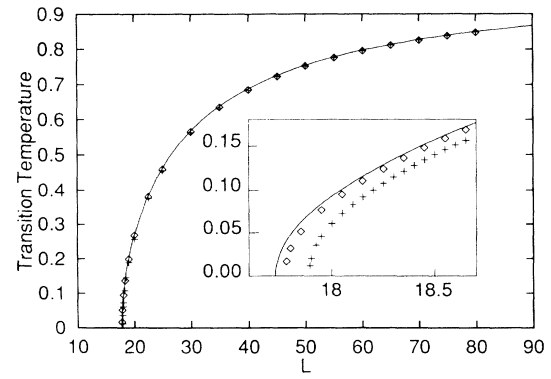

FIG. 8. The normalized transition temperature $T_c(d,l)/T_c(d,l{=}\infty)$, as a function of $L \equiv k_F l$ (l is the pair breaking impurity mean free path) for thicknesses $k_F d = \infty$ (solid line), $k_F d = 200$ (diamonds), and $k_F d = 50$ (crosses). The inset shows the detail of the region $T_c = 0$.

At constant d and l, and varying ξ_0, we find after carefully including terms of order (ω_0/E_F) in our calculations, that short ξ_0 superconductors deviate somewhat from Eq. (3.2): They are slightly less sensitive to pair breaking impurities than expected by straightforward application of the scaling formula. Note also that Eq. (3.2) has been proven approximately valid for infinite d-wave superconductors with a specific dispersion relation.[34] Therefore we believe that it is a rather general property of superconducting systems, treated within the second order self-consistent Born approximation.

In Fig. 9 we show the effect of pair breaking impurities on the results shown in Fig. 4. All parameters are the same as in Fig. 4, except that the mean free path is now finite. Two differences are apparent. First, the gap is, of course, reduced by the pair breaking impurities. Second, the geometric effects are rather broadened, which implies that their experimental observation may be hard to achieve.

Impurities change the value of $\xi(T)$. In standard superconductors one has, for nonpair breaking impurities,[2]

$$\xi_{\mathrm{GL}}(T) \sim \left(\frac{\xi_0 l_N}{1-t}\right)^{1/2}, \qquad (3.3)$$

where l_N is the mean free path. Equation (3.3) holds only when $l_N \ll \xi_0$. This assumption can *never* be satisfied in short ξ_0 materials, where one is in the regime l, $l_N \gg \xi_0$ even when the disorder is otherwise very significant (e.g., $l \sim 50$ Å). Superconductivity in these materials is then extremely robust with respect to pair breaking impurity scattering. As a result, impurities influence very little the shape of the order parameter near an interface. We show this in Fig. 10. There we plot $\Delta(z)$ near the surface of a superconductor with $\pi k_F \xi_0 = 20$ at a relatively high re-

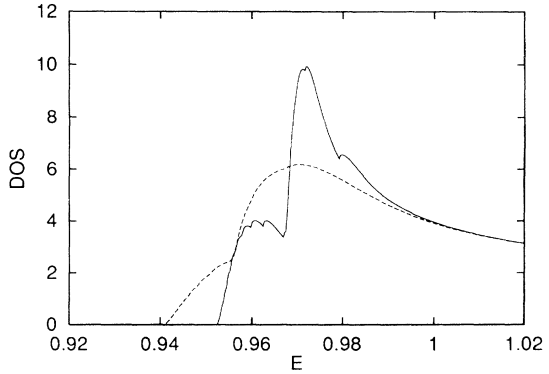

FIG. 9. As in Fig. 4, but with pair breaking impurities, $k_F l = 1 \times 10^4$ (solid line) and $k_F l = 1 \times 10^3$ (dashed line).

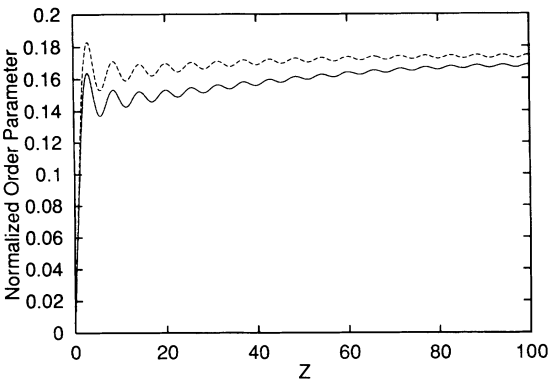

FIG. 10. $\Delta(z)/\Delta_0$ near the surface of a superconductor with $\pi k_F \xi_0 = 20$ at $t \equiv T/T_c(l) = 0.99$. The dashed line is for the clean case, and the solid line is for $k_F l = 50$.

duced temperature $t = 0.99$. The dashed line represents the results of Ref. 9 for the pure case ($t = T/T_c^0$) and the solid line the results for $k_F l = 50$ ($t = T/T_c$). Except for the overall reduction of the average value of $\Delta(z)$ (consistent with the previous discussion), the two curves are very similar. One can see that the solid curve rises to its bulk value slightly faster than its dashed counterpart, which can be interpreted as a slight decrease of the length $\xi(T)$ as the impurity concentration is increased. Note that Friedel oscillations are still present: Random impurities do not significantly affect the geometrical effects, although scattering from localized surface inhomogeneities would.

IV. CONCLUSIONS

We have performed a study of geometric and finite-size effects in short ξ_0 superconductors. We used a purely microscopic method, based on the Gor'kov equations in a slab geometry: they transform into a set of matrix equations, which we solve to obtain the order parameter and the density of states. We have introduced pair breaking disorder in a self-consistent way, using a perturbation expansion method, analogous to that of Abrikosov *et al.*,[16] generalized to our geometry.

Our results for the DOS indicate that an energy gap should be observed for a clean system, for all values of ξ_0. Moreover, this energy gap does not depend on the distance probed from the interface. In other words, a surface probe can indeed measure bulk properties of a superconductor. This may be especially significant for the case of short ξ_0 materials. The DOS does depend on the probing region (distance from the boundaries), but only slightly. For both long and short coherence length superconductors we found that the DOS in a slab of finite thickness, when integrated over a large transverse momentum area, exhibits size effects, manifested in the existence of many peaks in the DOS instead of a single one. This size effect is due to the variation in electron pairing, depending on their discrete momentum component orthogonal to the slab. This is a purely geometric effect, and does not significantly depend on ξ_0. Long ξ_0 films also exhibit quantum oscillations of the order parameter and the transition temperature. However, for short ξ_0 superconductors, the transition temperature and the average order parameter, as well as the energy gap, reach their bulk values with increased thickness monotonically from below. This difference is due to the fact that the condition $\xi_0 \ll d$ can never be reached in ordinary superconductors for any thickness d at which size effects are still relevant.

When pair breaking impurities are included, we find again that to a good approximation the energy gap is in all cases independent of the depth of the region probed near the interface. For a sample of finite thickness, we find that these impurities destroy superconductivity in the same way as in the bulk: the relative transition temperature $T_c(d)/T_c{}^0(d)$, where $T_c{}^0(d)$ corresponds to a clean slab, and $T_c(d)$ to a dirty slab, satisfies the same formula [Eq. (3.2)] to a high degree of accuracy. However, as expected, short ξ_0 superconductors are much less sensitive to impurity scattering. The dependence of T_c on thickness was found to be only minor in the short ξ_0 case. Finally, as in the clean case, we found that the OP in dirty short ξ_0 superconductors is mainly determined by the size of the system, and that its depletion at interfaces is still extremely small even at temperatures close to T_c. This is due to the fact that the coherence length ξ_0 is always much shorter than the mean free path l. These systems are never in a regime where the behavior of the system is dominated by impurity scattering, and in the gapless state the pair potential could still be large. This result could have important experimental consequences.

A consequence of our results is that (as in Ref. 9) the temperature dependent length $\xi(T)$ is relatively unimportant. Most of the change in $\Delta(z)$ takes place over a short length scale, and the relation between the DOS, as measured in tunneling and other probes, and the order parameter is approximately independent of the temperature. This result holds also in the presence of impurities.

We have assumed s-wave pairing. It would be easy to extend our calculations to other pairing states such as d-wave pairing. We do not expect that the results for the amplitude $\Delta(z)$ would change appreciably. The DOS would be different in the gap region if nodes were present, but our conclusions concerning its dependence on the lengths in the problem, particularly its weak dependence on z, should remain the same.

Our results are not without limitations. We have not included scattering from boundary roughness, nor the high anisotropy characteristic of many HTSC's, and we have worked within a weak coupling formalism. This last shortcoming is more difficult to remedy than the other two. Surface roughness scattering, for example, can be added using the method of Ref. 21. Anisotropy in both the effective mass and the coupling constants can also be easily included. Nevertheless, most of our results and conclusions are determined basically by geometrical constraints, and by the ratios of the different characteristic lengths in the problem as enumerated early in Sec. III. Hence, we expect them to be quite robust with respect to our specific assumptions. We believe that the fact that a large gap is experimentally observed in short ξ_0

superconductors, in both tunneling and photoemission experiments, is to a considerable degree a confirmation of the soundness of our approach. The finite-size effects in the DOS discussed in Sec. III, might be observable in tunneling data from experiments similar, for example, to those of Ref. 14. Last, but not least, our analysis shows that, when ξ_0 is small, one must think about the behavior of superconducting samples in a way which is not the same as that which most physicists have become used to through decades of experience with ordinary metallic superconductors. One must develop, so to speak, a new intuition.

In addition to the generalizations discussed above, an obvious extension of our work is to the study of structures, such as SN and SI multilayers[35] or granular superconducting materials. We plan to proceed with work along these lines.

ACKNOWLEDGMENTS

We would like to express our gratitude to M. T. Béal-Monod, S. W. Pierson, and M. G. Friesen for many useful conversations on the subject of this paper. We also thank A. M. Goldman and B. Batlogg for conversations on the experimental implications of this work. We acknowledge the Minnesota Supercomputer Institute for a grant of computer time. This project was supported in part by NSF under Grant No. DMR-8908094.

[1] J. Bardeen, L. N. Cooper, and J. R. Schrieffer, Phys. Rev. **108**, 1175 (1957).
[2] P. G. deGennes, *Superconductivity of Metals and Alloys* (Addison-Wesley, New York, 1989).
[3] A. McMillan, Phys. Rev. **170**, 481 (1968).
[4] W. J. Gallagher, Phys. Rev. B **22**, 1233 (1980).
[5] L. P. Gor'kov, Zh. Eksp. Teor. Fiz. **34**, 735 (1958) [Sov. Phys. JETP **7**, 505 (1958)].
[6] See, e.g., *Superconductivity*, edited by R. D. Parks (Dekker, New York, 1969), p. 174.
[7] J. G. Bednorz and K. A. Müller, Z. Phys. B **64**, 189 (1986).
[8] G. Deutscher and K. A. Müller, Phys. Rev. Lett. **59**, 1745 (1987).
[9] Branko P. Stojković and Oriol T. Valls, Phys. Rev. B **47**, 5922 (1993).
[10] C. G. Olson, R. Liu, A-B. Yang, D. W. Lynch, A. J. Arko, R. S. List, B. W. Veal, Y. C. Chang, P. Z. Jiang, and A. P. Paulikas, Science **245**, 731 (1989); J. M. Imer, F. Patthey, B. Dardel, W.-D. Schneider, Y. Baer, Y. Petroff, and A. Zettl, Phys. Rev. Lett. **62**, 336 (1989); R. Manzke, T. Buslaps, R. Calessen, and J. Fink, Europhys. Lett. **9**, 477 (1989).
[11] M. Lee, D. B. Mitzi, A. Kapitulnik, and M. R. Beasley, Phys. Rev. B **39**, 801 (1989); H. Ikuta, A. Maeda, K. Uchinokura, and S. Tanaka, Jpn. J. Appl. Phys. **27**, L1038 (1988); J-X. Liu, J-C. Wan, A. M. Goldman, Y. C. Chang, and P. Z. Jiang, Phys. Rev. Lett. **67**, 2195 (1991).
[12] T. Timusk and D. B. Tanner, in *Physical Properties of High Temperature Superconductors, II*, edited by D. M. Ginsberg (World Scientific, Singapore, 1990), pp. 620–629; T. Timusk and D. B. Tanner, in *Physical Properties of High Temperature Superconductors, III*, edited by D. M. Ginsberg (World Scientific, Singapore, 1992).
[13] M. J. Sumner, J.-T. Kim, and T. R. Lemberger, Phys. Rev. B **47**, 12 248 (1993).
[14] S. H. Tessmer, D. J. Van Harlingen, and J. W. Lyding, Phys. Rev. Lett. **70**, 3135 (1993).
[15] P. G. deGennes, Rev. Mod. Phys. **36**, 225 (1964).
[16] A. A. Abrikosov, L. P. Gor'kov, and I. E. Dzyaloshinski, *Methods of Quantum Field Theory in Statistical Physics* (Prentice-Hall, Englewood Cliffs, NJ, 1963).
[17] C. J. Thompson and J. M. Blatt, Phys. Lett. **5**, 6 (1963).
[18] See Eqs. (51.25) on p. 445 of A. L. Fetter and J. D. Walecka, *Quantum Theory of Many Particle Systems* (McGraw-Hill, New York, 1971).
[19] A. Sugiyama, J. Phys. Soc. Jpn. **15**, 965 (1960).
[20] V. Z. Kresin and B. A. Tavger, Zh. Eksp. Teor. Fiz. **50**, 1689 (1966) [Sov. Phys. JETP **23**, 1124 (1966)].
[21] Z. Tešanović and O. T. Valls, Phys. Rev. B **33**, 3139 (1986).
[22] A. V. Chaplik and M. V. Entin, Zh. Eksp. Teor. Fiz. **55**, 990 (1968) [Sov. Phys. JETP **12**, 1242 (1961)].
[23] The quantity $N(z, k_\perp, E)$ is properly speaking the spectral density, which is commonly referred to as the DOS.
[24] J. C. Phillips, *Physics of High-T_c Superconductors* (Academic Press, San Diego, 1989).
[25] In STM measurements the probability for tunneling electrons with large momentum components parallel to the plane of a sample vanishes exponentially.
[26] However, if d depends on x, y directions, information about this dependence can be obtained from STM measurements.
[27] S. W. Pierson and Oriol T. Valls, Phys. Rev. B **45**, 2458 (1992).
[28] M. Yu, M. Strongin, and A. Paskin, Phys. Rev. B **14**, 996 (1976).
[29] D. S. Falk, Phys. Rev. **132**, 157 (1963).
[30] B. G. Orr, H. M. Jaeger, and A. M. Goldman, Phys. Rev. Lett. **53**, 2046 (1984).
[31] We find that for the results shown in Fig. 6 one has $\xi(T) > \xi_{GL}(T)$.
[32] K. Maki, in *Superconductivity*, edited by R. D. Parks (Dekker, New York, 1969).
[33] T. Giamarchi, M. T. Beal-Monod, and Oriol T. Valls, Phys. Rev. B **41**, 11 033 (1990).
[34] R. J. Radtke, K. Levin, H.-B. Schüttler, and M. R. Norman, Phys. Rev. B **48**, 653 (1993).
[35] Branko P. Stojković and Oriol T. Valls, Proceedings of the International Low Temperature Conference LT20 [Physica C (to be published)].